Development of Metallic Superconductors in Japan

Kyoji Tachikawa
Faculty of Engineering, Tokai University
4-1-1, Kitakaname, Hiratsuka, Kanagawa 259-1292, Japan
E-mail: tacsuper@keyaki.cc.u-tokai.ac.jp

***Abstract* – This article overviews the development of metallic superconductors in Japan covering different kinds of alloys, intermetallic compounds and MgB_2. Metallic superconductors have opened many new application areas in science and technology. Japan has been one of the leading countries in the world, both in the research and development and in large-scale manufacturing of metallic superconductors.**

Received April 1, 2011; accepted April 27, 2011. Reference No. RN20, Categories 2, 5, 13.

***Keywords* –alloys, intermetallic compounds, MgB_2, fabrication process, microstructure, superconducting wire, superconducting cable, superconductor performance, superconducting magnet, application of superconductivity**

I. INTRODUCTION

Just half a century has passed since the fabrication of high-field Nb_3Sn wire via powder-in-tube process by J.E. Kunzler in 1961 [1]. Since then metallic superconductors made significant progress becoming an innovative tool in different areas, such as medical instruments, energy systems, transportation systems, *etc*. At present the share of commercial production of metallic superconductors is estimated to be over 95 % of the total including cuprate superconductors. Metallic superconductors have made progress through intimate linkage among areas of new material research, process development and application technologies. Development of new materials opens a new application field, while application projects improve the material processing technologies. Thus material and application have made progress by maintaining a close interrelation. This article outlines the historical progress and recent developments of metallic superconductors in Japan. Some of the major

contributions are the effect of Cu on the synthesis of V_3Ga governing the bronze process, initiation of the internal Sn process, Ti doping effect on the performance of Nb_3Sn, development of Nb_3Al wires, and the discovery of MgB_2 superconductors.

II. Nb-Ti AND RELATED ALLOY SUPERCONDUCTORS

Nb-Ti wires are now widely used for generating magnetic fields up to 9 T at 4.2 K and 11 T at 1.7 K. However, Nb-Zr alloy wire was developed first, starting in 1960, as a candidate for superconducting magnet use [2]. Studies on metallic superconductors in Japan have been initiated in 1962 on Nb-Zr alloy wires at the National Research Institute for Metals (NRIM)[1]. Nb-Zr alloy has a slightly higher transition temperature T_c of 10.8 K and a slightly lower upper critical field B_{c2} (4.2 K) of 10.5 T than those of the Nb-Ti alloy. About 1 km long wires, 0.25 mm in diameter, were fabricated from ingots containing 25 – 50at% Zr. Figures 1(a) and (b) show electron micrographs of Nb-50 at% Zr alloy wires after the eutectic separation (β Nb + β Zr) at 785℃ and the eutectoid separation (β Nb + α Zr) at 560℃, respectively [3]. The critical current density J_c of Nb-Zr wire is appreciably enhanced by these phase separations. Our report on the J_c improvement by the structure modification in metallic superconductors may be the first one on this topic. After a thick electroplating of Cu for stabilization, many small Nb-Zr alloy magnets generating fields of 5 to 6T were made. However, about 1965, Nb-Zr wires were replaced by Nb-Ti wires, which are easily fabricated together with a Cu matrix into a multifilamentary configuration necessary for the electromagnetic stabilization.

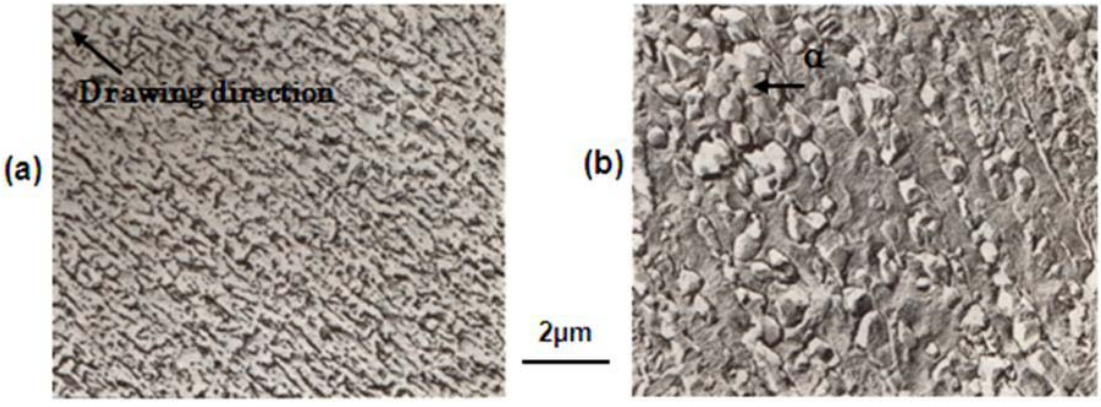

Fig.1. Electron micrographs of the longitudinal cross-section of Nb-53wt%Zr wire. (a) Heat treated at 785℃ for 25h (β_{Nb}+β_{Zr} separation), (b) heat treated at 560℃×100h (βNb+αZr separation) [3].

[1] Renamed in 2001; now the National Institute for Material Science (NIMS).

The Nb-Ti alloy is suitable for mass production since large and homogeneous ingots can be produced with enough mechanical tolerance to be fabricated into thin wires. Nb-Ti wires still keep a major share among superconducting wires throughout the world. In Japan, industrial production of Nb-Ti wires started at Furukawa Electric Co. Ltd. in 1967, at Hitachi Cable Ltd. in 1968 and at Kobe Steel Ltd. (now transferred to JASTEC) in 1977. At present these three companies are still major suppliers of Nb-Ti wires in Japan. In the early stage of the Nb-Ti wire development, ternary alloy wires, e.g. Nb-Ti-Zr (at Hitachi Ltd.), Nb-Ti-Ta (Mitsubishi Electric Co.) and Nb-Ti-Hf (at NRIM) were studies in Japan. A slight improvement in the performance at 1.7 K was reported in these ternary alloys.

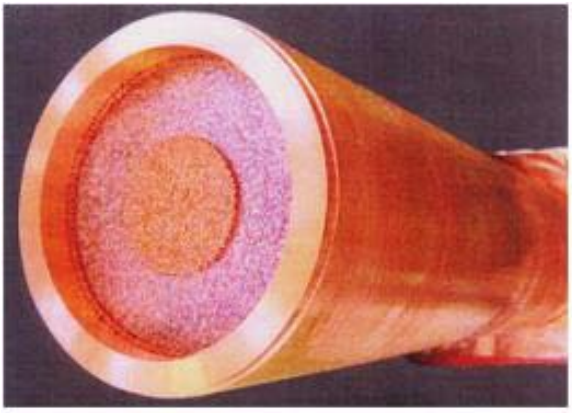

Fig.2. An assembled Nb-Ti billet for extrusion. Outer diam.: 236.5mm, Number of Nb-Ti cores: 8500, Center: Cu rods [4].

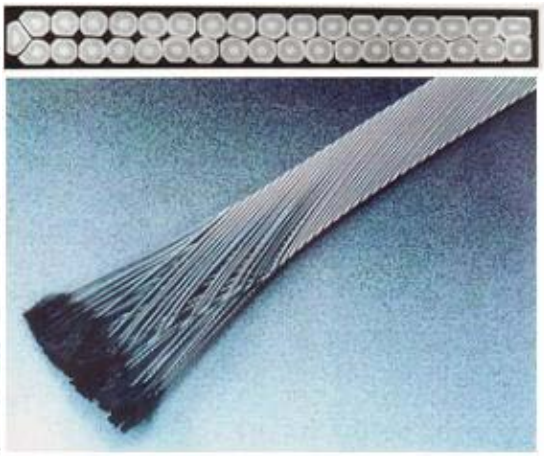

Fig.3. Rutherford-type Nb-Ti cable for LHC. Width: ～ 15mm, Thickness: ～ 1.5mm, Number of composite strands : 36 [4].

Figure 2 is a recent example of a Nb-Ti billet for LHC (Large Hadron Collider) prepared at Furukawa [4]. The billet is composed of 8500 single core Nb-Ti / OFHC Cu composites. The billet is fabricated into an about 50 km long 0.825 mm ϕ wire through extrusion and subsequent drawing. Intermediate annealing steps are inserted during the drawing to introduce α-Ti precipitates which are effective pinning centers to enhance the J_c in Nb-Ti wires. The resulting wire contains 6 μm $\phi \times 8500$ Nb-Ti filaments, the Cu ratio and the twist pitch being 1.95 and 15 mm, respectively. The wire (strand) exhibits a non-Cu J_c of 2300 A/mm^2 at 4.2 K and 6 T. Finally, Rutherford cables shown in Figure 3 composed of 36 strands have been produced for LHC. Nb-Ti wires are being widely used for MRI, and the Japanese MAGLEV train shown in Figure 4 [5], energy storage, semiconductor crystal growth, fusion, high energy accelerators, *etc*.

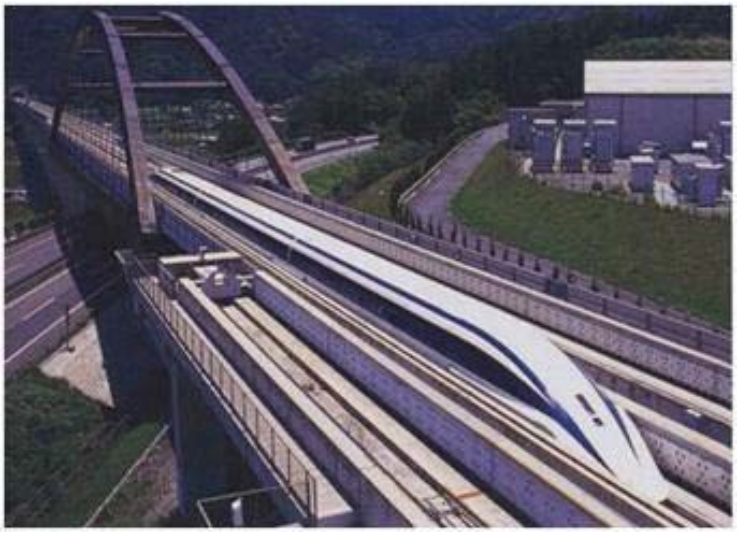

Fig.4. In 2008, the superconducting magnetically levitated train reached the speed of 581km/h [5].

The introduction of artificial pinning centers, such as fine Nb lamellae, to Nb-Ti wires has been studied in Japan, in 1990s [6]. Artificial pinning centers produce more uniform flux pinning than α-Ti precipitates in Nb-Ti wires. Also in 1990s, the development of Nb-Ti wires for AC use has been performed in conjunction with the superconducting generator project in Japan. In the Nb-Ti wires for AC use, the filament diameter is reduced to 0.1 μm to minimize the hysteresis loss. Figure 5 illustrates an example of an AC Nb-Ti strand containing 0.1 μm ϕ × 1,023,033 filaments embedded in a Cu-Ni matrix [7]. The central part and the outer sheath of the wire is pure Cu. In the Nb-Ti wire with Cu-30 wt% Ni-0.9 wt% Mn matrix, an AC loss as low as 17 J /m^3 (at $\pm$0.5 T) has been achieved [7]. The cable was assembled of 36 strands, such as that shown in Figure 5, to increase the current capacity of the cable.

Furthermore, Nb-Ti wires stabilized by Al have been developed in Japan. The LHD (Large Helical Device) magnet in the National Institute for Fusion Science was wound by totally 36 km-long Al stabilized Nb-Ti conductors carrying ~50 kA at 4.4 K and 7 T [8]. Another Al stabilized Nb-Ti conductor was used for the ATLAS detector magnet of the LHC facilities [9], as well as for the superconducting ring cyclotron in RIKEN [10]. Furthermore the light weight Al stabilized Nb-Ti wire has been used for the spectrometer in the Bess-Polar balloon [11].

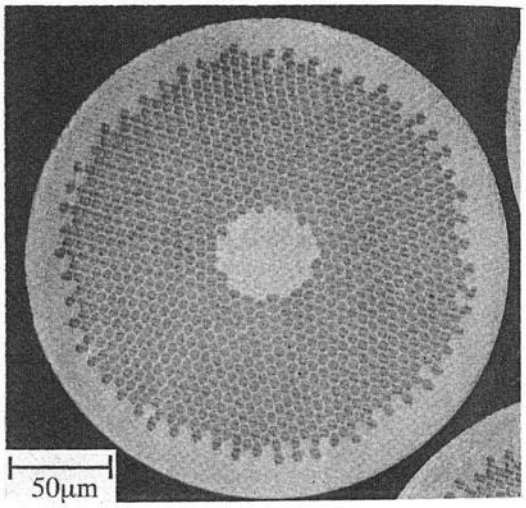

Fig.5. A cross section of AC Nb-Ti wire (strand) containing $\sim 10^6$ fine filaments [7].

III. Nb_3Sn AND V_3Ga WIRES

Both Nb_3Sn and V_3Ga are A15-type compounds, which are indispensable to generate fields over 10 T at 4.2 K. They have been fabricated into multifilamentary wires, analogous to Nb-Ti wires, through the so-called bronze process. Various types of Nb_3Sn wires are now being widely used in NMR, fusion and other magnets, and became one of the key materials in science and technology. A trigger study of the effect governing the bronze process, i.*e*., the effect of Cu on the synthesis of the V_3Ga compound, has been reported in 1967 [12]. Nb_3Sn and V_3Ga are in this respect like brother materials among the A15 compounds.

In the preparation of V_3Ga, a V substrate tape continuously passes through a molten Ga bath forming the Ga-rich compound layers on both sides of the tape. A small amount of Cu addition to molten Ga changes the diffusion mode for the synthesis of V_3Ga layer from a grain boundary one to a bulk one. Cu is soluble to the Ga-rich compound, however is not incorporated in the V_3Ga layer and accumulates at the diffusion boundary decreasing appreciably the formation temperature of V_3Ga as illustrated in Figure 6. The areal fraction of the V_3Ga layer with fine grains and high J_c is much increased by this procedure.

Here begins the story of finding the effect of Cu on the synthesis of V_3Ga layer. I plated a thin layer of Au, Ni and Cu on the surface of tape specimens. The purpose was to protect the specimen against oxidation when they were heat treated under an Ar atmosphere. I found that all of these elements significantly enhance the formation of

V_3Ga layer. However Au and Ni are incorporated into V_3Ga layers resulting in a drastic deterioration of T_c and other superconducting parameters of the tapes. This may have been due to the fact that Au and Ni forms A15 V_3Au and V_3Ni. Only Cu does not penetrate into the V_3Ga layer as described above. When I was measuring I_c of the specimen, I was much surprised by the abrupt increase of its value from a few amperes to a hundred amperes. We then found a similar effect of Cu in the synthesis of Nb_3Sn tapes. The patent describing the effect of Cu on the promotion of V_3Ga and Nb_3Sn synthesis was filed in 1966 [13].

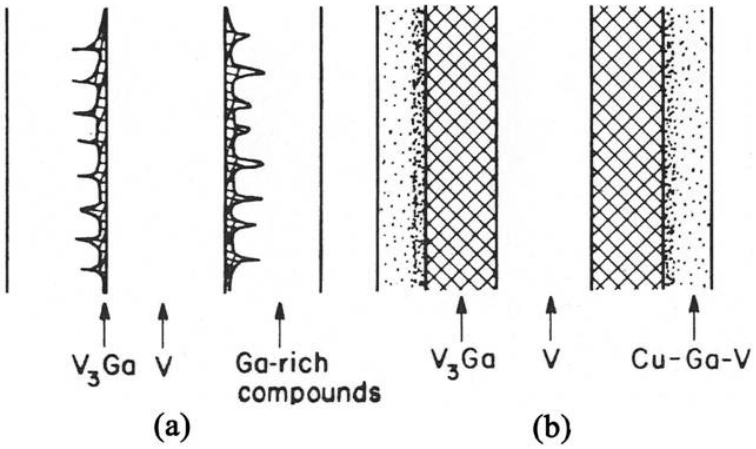

Fig.6. Formation of V_3Ga layer by a diffusion reaction between V and Ga. (a) Diffusion at 800℃ without Cu addition, and (b) at 700℃ with Cu addition. The dots represent the Cu in the Cu-Ga-V ternary alloy [12].

The V_3Ga tape exhibits an appreciably better performance than the pure Nb_3Sn tape in fields above 15T. In 1975, the 17.5 T superconducting magnet system shown in Figure 7 was made by using a Nb_3Sn outer section and a V_3Ga inner section [14]. It held the world record in the field intensity of superconducting magnets for ~10 years. However, tape conductors have a handicap of the so-called low-field instability when the field is applied perpendicular to the tape surface.

As an extension of the effect of Cu addition to Ga, the multifilamentary V_3Ga wire was fabricated from the composite of Cu-Ga matrix containing 15 – 20 at % Ga and V cores [15]. After the heat treatment at 600 – 650℃, Ga in the matrix selectively diffused to the V cores, and only V_3Ga layers were formed around V cores. This process realized A15 compound wires stable under normal and time varying field. The first commercial multifilamentary V_3Ga wire was produced by the Furukawa Electric in 1972 [16]. Subsequently, a 50 mm bore 13 T magnet for laboratory use was

Fig.7. 17.5T superconducting magnet system operated at NRIM [14].

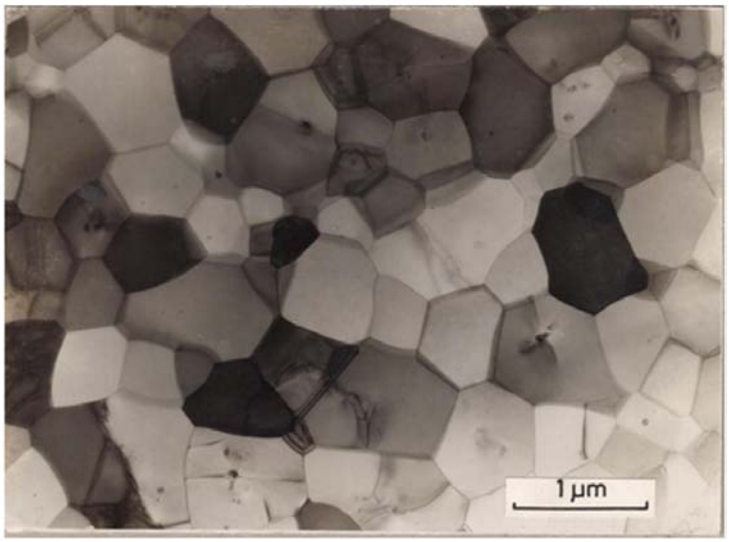

Fig.8. A transmission electron micrograph of the V_3Ga layer formed at 700℃ for 48h [17].

made using the multifilamentary V_3Ga wire.

Meanwhile, at NRIM we performed a fundamental transmission electron microscopy study on the microstructure of the V_3Ga tape, such as shown in Figure 8. There are almost no precipitates and dislocations in V_3Ga grains. This was the first important report indicating that the major flux pinning centers in A15 compounds were grain boundaries [17]. Therefore, the Cu addition, which decreases the formation temperature of V_3Ga thus resulting in fine grains, plays a significant role in enhancing J_c.

In early 1970's, the process of fabricating multifilamentary Nb_3Sn wires using a bronze matrix has become common throughout the world. As a modification of the bronze process, the internal tin (IT) process using a triple composite of Cu matrix, Sn

and Nb cores has been initiated at Mitsubishi Electric Co. in 1974 [18]. Hard and brittle V_3Ga and Nb_3Sn compounds have been successfully fabricated into multifilamentary wires like those of ductile Nb-Ti alloys, at a level approaching industrial stage.

Figure 9 schematically illustrates the bronze process and IT process with a small amount of Ti addition to the matrix. Figure 10 depicts typical bronze ingots prepared

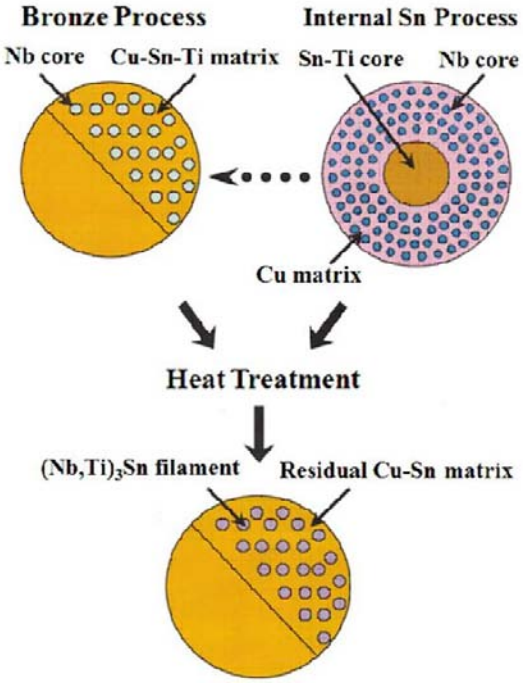

Fig.9. Schematic illustration of bronze and internal Sn (IT) process.

Fig.10. Typical bronze ingots for Nb_3Sn wires (Courtesy of Osaka Alloying Works Co., Ltd.) [19].

at Osaka Alloying Works [19]. Diameter, length and weight of the ingot are ~200 mm, ~800 mm and ~250 kg, respectively. Typically 19 or 37 holes are drilled in the ingot, in which Nb cores are inserted. The composites are fabricated to hexagonal rods which are stacked in a Cu cylinder with Ta or Nb barrier inside, the purpose of which is to protect stabilizing Cu from any Sn diffusion. The multi-rod stacked billet is hot extruded, and drawn into a multifilamentaly wire. The wire is finally heat treated at ~675℃ for ~200 h to form Nb_3Sn layers around Nb cores.

Addition of different elements to Nb_3Sn has been investigated aiming at the improvement in its performance. We found the addition of Ti to be the most favorable [20]. Table 1 summarizes the effect of the Ti addition to the bronze on T_c, Ti inclusion in Nb_3Sn, the upper critical field B_{c2} (4.2 K), and the normal state resistivity ρ_n. The

B_{c2} (4.2 K) of Nb_3Sn is effectively enhanced from 19.5 T to 26.4 T. This may be caused by the increase in ρ_n [21]. Excessive Ti addition decreases B_{c2} due to the decrease of T_c. Titanium may be added either to the bronze or Nb cores, however, the addition to the bronze is technically preferable. Originally, I intended to improve the mechanical strength of the residual bronze after the heat treatment by the Ti addition. Unfortunately Ti is entirely incorporated into the Nb_3Sn layer or accumulates at the Nb_3Sn/bronze boundaries, and is not effective for the reinforcement of the bronze. Fortunately the Ti incorporation appreciably improves the high-field performance of Nb_3Sn as described above. A small amount of Ta may be added to Nb cores for the B_{c2} enhancement [22].

Table1 T_c, Ti concentration in Nb_3Sn layer, B_{c2}(4.2K) and ρ_n of Nb/Cu-7.0 at.% Sn-Ti wire reacted at 750℃ for 100h [20].

Specimen (at%)	T_c (K)	Ti content in Nb_3Sn (at%)	B_{c2} (T)	ρ_n ($\mu\Omega$m)
Nb/Cu-7Sn	17.2	0	19.5	0.08
Nb/Cu-7Sn-0.2Ti	17.7	1.05	25.1	0.21
Nb/Cu-7Sn-0.35Ti	17.5	1.60	26.4	0.33
Nb/Cu-7Sn-0.5Ti	16.2	2.71	26.1	0.41
Nb/Cu-7Sn-1.0Ti	15.6	3.65	24.8	0.55
Nb/Cu-7Sn-1.5Ti	15.2	3.92	24.2	0.58

In 1990's the Sn concentration in the bronze has been increased from 13 wt% to 16wt%, which has doubled the non-Cu J_c of the wire at 4.2 K and 20 T. Many high-field NMR magnets have been made by Ti-doped bronze-processed Nb_3Sn wires. Figure 11 is an example of a NMR magnet developed in Japan using 16 wt% Sn-0.3 wt% Ti bronze Nb_3Sn wire, which generated 21.9 T at 1.5 K in a persistent current mode [23]. Furthermore a variety of refrigerator-cooled magnets, vertical, horizontal and split pairs, wound using bronze-processed Nb_3Sn wires have been introduced in the commercial market. The magnet shown in Figure 12 generates 15 T in a 171 mm room- temperature bore [24].

Figure 13 is an example of the cross-section of a bronze-processed Nb_3Sn wire developed in Japan for ITER (the International Thermonuclear Experimental Reactor) [25]. A large number of wires are encased in a long SUS316LN jacket together with Cu wires to prepare a CIC (cable-in-conduit) conductor. Figure 14 shows the 1km-long jacketing facility [26]. In addition Nb_3Sn wires for AC use have been developed through the bronze process. The filament diameter in the wire is reduced to 0.2 μm minimizing the hysteresis loss. In the AC Nb_3Sn wires the Sn concentration

Fig.11. 930MHz NMR magnet installed at NIMS [23].

Fig.12. Refrigerator-cooled superconducting magnet [24].

of the bronze is decreased,instead a small amount of Ge is added to suppress the filament coupling. In such ultra-thin filament Nb_3Sn wires the heat treatment temperature is decreased to 500℃－550℃. Moreover the J_c of the wire does not degrade under the bending strain of nearly 4 % which enables the react and wind process for the magnet winding. A 50mm bore 2 T Nb_3Sn magnet was successfully operated at 53 Hz with an AC loss of ~0.013 % of the coil energy [27].

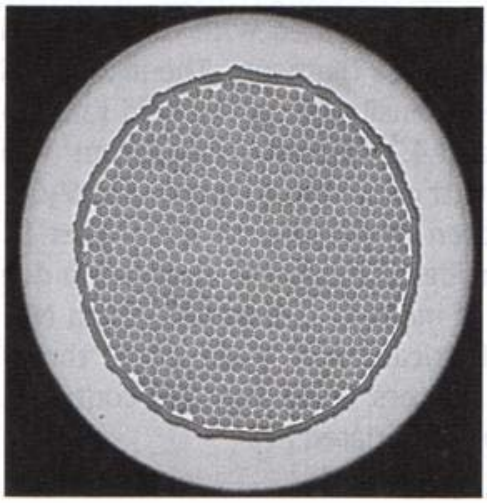

Wire diam. (with Cr plating)	0.826 mm
Twist pitch	15.0 mm
Bronze composition (wt%)	Cu-15.5 Sn-0.3Ti
Filament composition (wt%)	Nb-1.0 Ta
Filament diameter	3.0 μm
No. Filament	19×583=11,077
Cu/non Cu ratio	1.0
Barrier material	Nb
non Cu J_c @ 12 T, 4.2 K	820 A/mm^2
n-value @ 12 T, 4.2 K	30.0
Hysteresis loss @ ± 3 T, 4.2	620kJ/m^3

Fig.13. Cross-section and specification of the bronze processed $(Nb,Ti)_3Sn$ conductor (Courtesy of Japan Atomic Energy Agency) [25].

Fig.14. Aerial view of the 1km-long jacketing facility for the ITER conductor (Courtesy of Japan Atomic Energy Agency) [26].

The IT process is also used in fabrication of wires for fusion projects, including ITER. The principle of the IT process has been shown in Figure 9. The bronze has the Sn solubility limit of ~15.8 wt%, while a larger Sn fraction in the matrix may be possible in the IT process, resulting in an increase of the non-Cu J_c in the wire. Since the IT processed wire is composed of three components, a variety of cross-sectional designs are possible. A small amount of Ti is added to the Sn core for enhancing B_{c2} similar to the bronze process. In the fabrication of bronze processed wires frequent intermediate annealings are required due to the work hardening of the bronze, while the IT process does not require them resulting in a much shorter fabrication time.

A disadvantage of the IT process is the melting of Sn during the extrusion. A temporary core such as Cu is used at the extrusion, which is replaced by a Sn core after the extrusion. A complex and longer heat treatment is required in the IT process to convert Sn core and Cu matrix to the bronze matrix. The Sn core becomes a hole after the heat treatment. Generally the *n* value and the longitudinal homogeneity of the wire are better in the bronze processed wires. In the IT wires Nb_3Sn filaments tends to cause bridging after the heat treatment, which increases the AC loss. Thus IT wires show larger non-Cu J_c and AC loss than bronze processed wires.

The Mitsubishi Electric Co. developed an IT processed wire with a modified Nb filament arrangement to reduce the AC loss. The cross-section and the specification of the wire are shown in Figure 15. The wire achieved a high non-Cu J_c of 1150 A/mm^2 at 4.2 K and 12 T, and a relatively low AC loss ($\pm$3T) of 301 kJ/m^3 [28]. The IT Nb_3Sn wires produced in the Mitsubishi Electric Co. were used for the construction of KSTAR (Korea Superconducting Tokamak Advanced Research) facilities. In ITER facilities a total of 502 tons of Nb_3Sn wires fabricated by both bronze and IT process are required to generate 13 T necessary for the plasma confinement.

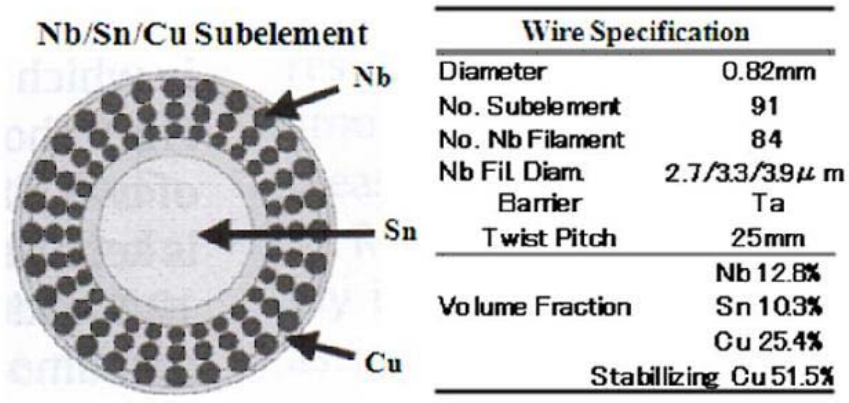

Fig.15. Cross-section of a sub-element with a modified Nb filament arrangement, and specifications of the wire using the sub-elements [28].

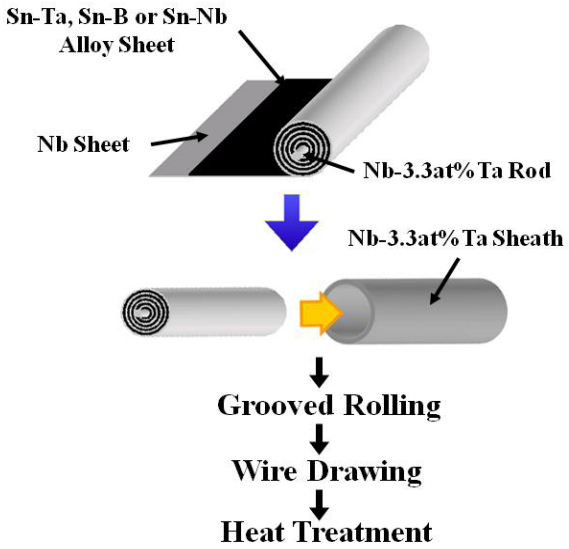

Fig.16. Schematic illustration of the JR process for the fabrication of Nb_3Sn wires.

Recently, at Tokai University we developed the Jelly Roll (JR) process to fabricate Nb_3Sn wires with high performance [29]. A Sn-based alloy sheet, such as Sn-Ta, Sn-B and Sn-Nb, is laminated with a Nb sheet to form a JR composite, which is encased in a sheath and then fabricated into a wire as illustrated in Figure 16. After the heat treatment at 725℃－750℃ the wire shows an offset T_c of 18.1 K with a transition width of less than 0.1 K, an offset B_{c2} (4.2 K) of 26.5 T, and a non-Cu J_c of 150 A/mm^2 at 4.2 K and 22 T. These performance parameters of the wire seem to approach the top of what was attained in various Nb_3Sn wires. Uniform and stoichiometric Sn concentrations in the Nb_3Sn layers may yield an overall improved performance of the JR wires.

IV. Nb_3Al AND OTHER COMPOUND WIRES

Nb_3Al has been considered as an alternative to Nb_3Sn for high-field and large-scale applications, such as fusion and high-energy particle accelerators, because excellent strain tolerance has been demonstrated for Nb_3Al. Unfortunately, the formation of unwanted ternary compounds including Cu does not allow the bronze process to be applied in the fabrication of Nb_3Al wires. Furthermore, the stoichiometric composition, a key to achieving a high T_c and a B_{c2} in Nb_3Al, is only obtainable at a very high temperature, nearly 2000℃. Such high-temperature heat treatment yields coarse-grained Nb_3Al with poor J_c. At lower temperatures, intermediate compounds richer in Al, $NbAl_3$ and Nb_2Al, are predominantly formed. Consequently, various fabrication processes have been developed in Japan to reconcile the desired fine grain structure with stoichiometry.

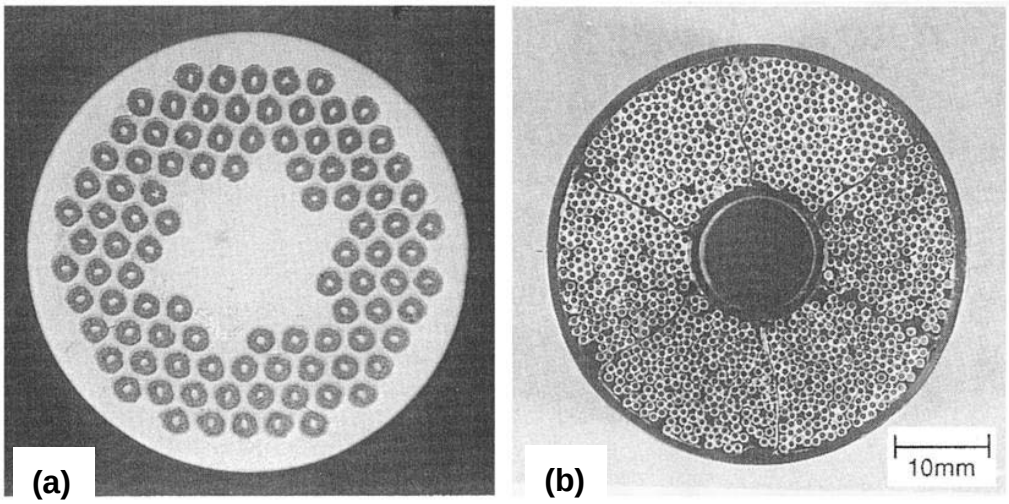

Fig.17. Cross-sections of JR processed Nb_3Al wires. (a) A strand 0.81 mm in diameter with 96 sub-elements [31], (b) a CIC conductor with 1152 strands shown in (a) [32].

The Nb/Al JR process, that was originally developed in Italy [30] and was further developed in Japan, has become the most common and reliable method of producing long-length Cu-matrix Nb/Al wire. In the JR process, laminated sheets of Al and Nb were wound around a Cu central rod to form a composite which was encased in a Cu sheath and then drawn into a JR sub-element. Figure 17 shows a cross-section of the Nb_3Al strand containing 96 sub-elements [31], as well as that of the CIC conductor with 1152 strands [32]. The JR wire is reacted to form Nb_3Al by diffusion heat treatments at a practical temperature around 750℃. A non-Cu J_c of ~1000 A/mm^2 has been obtained at 4.2 K and 12 T in the strand [31]. The Japan Atomic Energy

Association developed the Cu-stabilized JR Nb_3Al conductor as a candidate for the fusion magnets. The piece-length of the JR strand reached 11 km. Using such strands, CIC conductors with a current capacity of 46 kA @ 13 T have been developed for the Nb_3Al insert coil as a part of the ITER central solenoid model coil [32].

As long as the diffusion reaction temperature between Nb and Al is below 800℃, the B_{c2} (4.2 K) of the JR Nb_3Al conductor is, however, lower than 22 T. Thus, as a next step, an attempt was made to perform the straightforward diffusion reaction of Nb/Al composites at a high temperature over 1800℃ with continuous laser or electron beam irradiation techniques [33]. This improved much the B_{c2} (4.2 K), but traded off the high J_c in lower fields due to the unavoidable excess grain coarsening of the Nb_3Al phase. A J_c (irradiated part) of ~300 A/mm^2 has been obtained at 4.2 K and 25 T through this process. Nearly the same value was, however, obtained at 10 T [33].

At NRIM we demonstrated early on that the transformation process can reconcile the stoichiometry and fine grain structure requirements so that the J_c of Nb_3Al is significantly improved over the whole range of magnetic fields. In this process, the stoichiometric Nb_3Al forms by a transformation to A15 phase from a metastable bcc Nb solid solution extending to 25 at%Al $(3Nb \cdot Al)_{ss}$. Since the transformation requires only a change in crystal structure and not that in composition, the A15 Nb_3Al transformed from $(3Nb \cdot Al)_{ss}$ has a high stoichiometry as well as fine grains. We made two attempts to prepare the $(3Nb \cdot Al)_{ss}$ wires.

At first, the liquid quenching and transformation process has been applied, in which an arc-melted liquid was quenched on a Cu substrate heated at ~500℃ [34]. The heated substrate results a better spread of the melt which effectively increase the quenching rate. Besides $(3Nb \cdot Al)_{ss}$, $(3Nb \cdot Al_{1-x}Ge_x)_{ss}$ and $(3Nb \cdot Al_{1-x}Si_x)_{ss}$ were obtained by the liquid quenching from the melt up to x=0.3. A partial substitution of Ge or Si improves the performance of Nb_3Al. Then the $(3Nb \cdot Al)_{ss}$ was heat treated at ~800℃ for short time to transform into the A15 phase. The transmission electron micrography on the liquid-quenched and annealed $Nb_3(Al_{0.8}Ge_{0.2})$ specimen revealed that the average grain size can be as small as 30nm [35]. The T_c of the liquid quenched and annealed Nb_3Al and $Nb_3(Al,Ge)$ specimens were 18.2 K and 19.4 K, respectively. A quite high J_c of ~1000 A/mm^2 at 4.2 K and 20 T was obtained in these specimens [35].

Subsequently, we fabricated Nb_3Al-based tapes by dropping the melt on a Cu substrate tape moving at high-speed of ~10 m/sec [35]. The $(3Nb \cdot Al)_{ss}$ layers, about 20 μm thick and 3 mm wide, tightly spread on the Joule-heated Cu tape. Several meters long Nb_3Al-based tapes with Cu stabilizing substrate were prepared by a

laboratory scale apparatus.

For the fabrication of longer Nb_3Al wires through the transformation process, NRIM has been developing since 1994 the RHQT (Rapid-Heating, Quenching and Transformation) process [36]. The JR processed multifilamentary precursor wire several hundred meters in length, have been reel-to-reel ohmic-heated to ~1950℃ where bcc solid solution extends to 25at.%Al, quenched into a molten gallium bath at ~50℃, and transformation-annealed at ~800℃ to form Nb_3Al phase. The RHQT process is schematically illustrated in Figure 18. The moving speed of the precursor wire is ~20m/min. In contrast to the conventional JR wire described before, the matrix material is Nb instead of Cu. One of the important characteristics of the RHQT Nb_3Al is ductility of the bcc $(3Nb \cdot Al)_{ss}$ at room temperature, because this enables cabling and winding before the transformation annealing. Utilizing the ductile nature of $(3Nb \cdot Al)_{ss}$ at room temperature, Cu stabilizer can be incorporated into a wire after quenching by mechanical cladding method. Moreover the J_c of the wire after the annealing is nearly doubled by the drawing at room temperature in the bcc state. Alternatively, the stabilizing Cu may be electroplated on the wire after the transformation heat treatment.

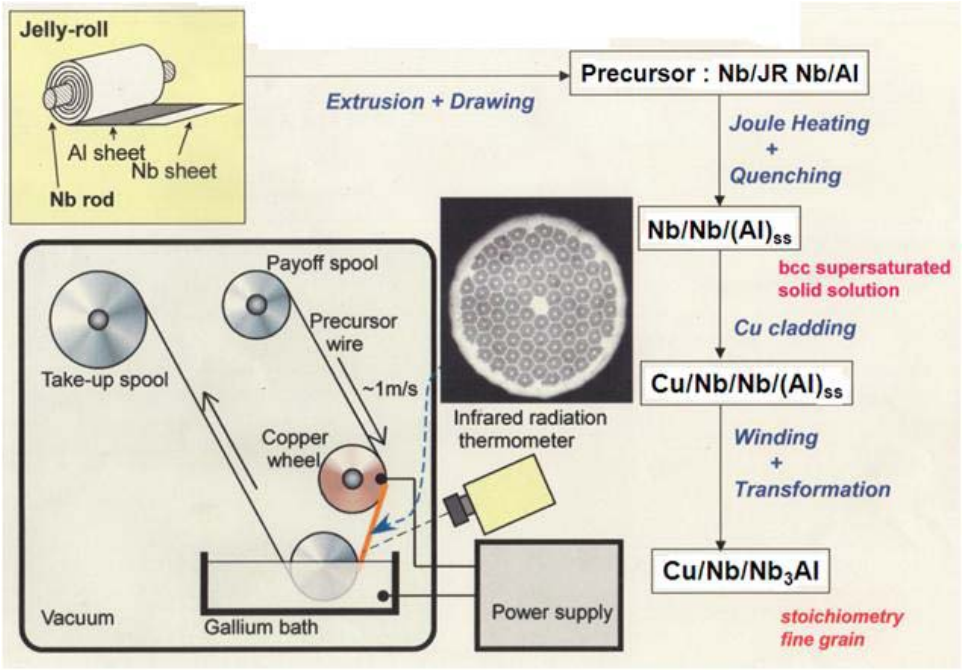

Fig.18. Continuous rapid heating and quenching apparatus for Nb_3Al wires. Outline of the entire process in also illustrated [36].

Figure 19 presents the non-Cu J_c versus magnetic field curves of two Nb_3Al wires together with those of three recent Nb_3Sn wires. The RHQT Nb_3Al wire shows the

highest non-Cu J_c at 4.2K and 20T of all the wires shown in Figure 19, much improved compared to the ordinary JR processed Nb_3Al wire. A reliable production technique has been established for a km-long RHQT Nb_3Al wire. A test insert coil of RHQT Nb_3Al wire shown in Figure 20 successfully generated 19.5 T at 4.2 K in a back up field of 15 T generated by a NbTi/Nb_3Sn magnet [36]. Furthermore the RHQT Nb_3Al cables are being developed for particle acceleration magnets, because of better strain tolerance than that of Nb_3Sn wires [37].

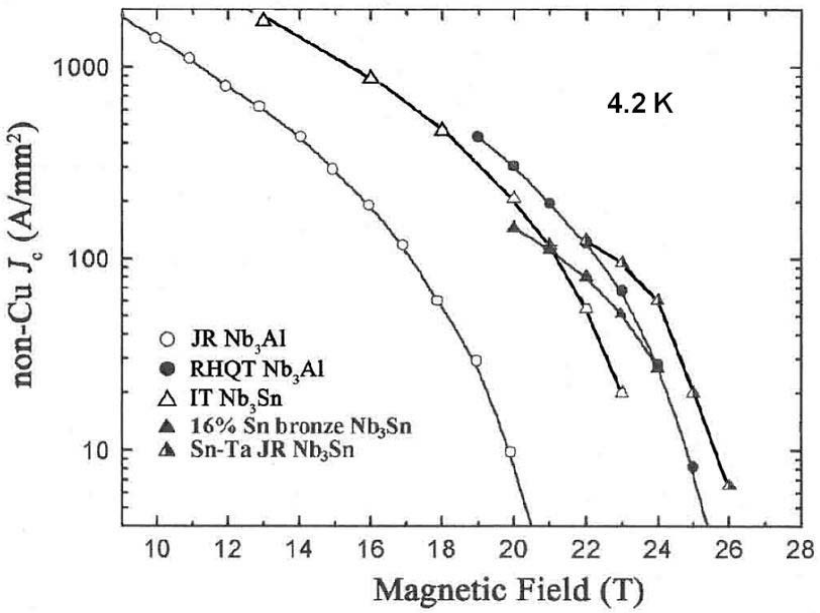

Fig.19. Comparison of non-Cu J_c versus magnetic field curves of Nb_3Al and a few recent Nb_3Sn wires.

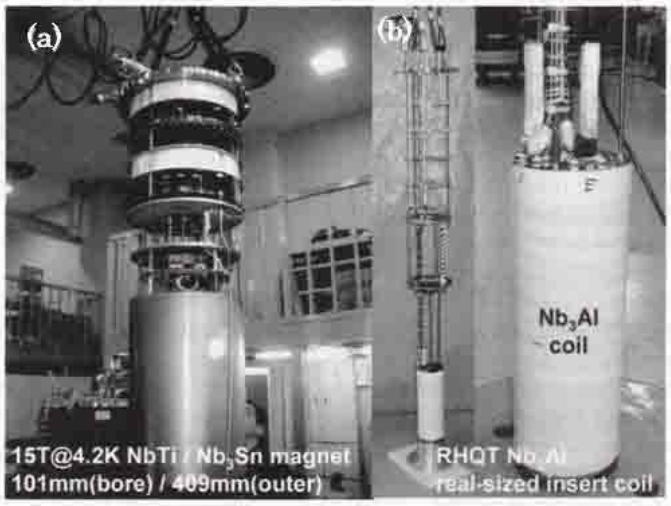

Fig.20. Overviews of (a) back-up Nb_3Sn magnet and (b) RHQT Nb_3Al insert coil [36].

At NRIM, we also studied the fabrication of C15 (Laves) crystal type compounds, which have unique characteristics. Laves type compounds with T_c exceeding 10 K are ternary V_2(Hf, Zr) (10.1 K), (V, Nb)$_2$Hf (10.4 K) and (V, Ta)$_2$Hf (10.0 K) [38]. These compounds have high B_{c2} (4.2 K) of 24 – 26 T in spite of their relatively low T_c. Furthermore, Laves type compounds have a distinct mechanical advantage by not being so hard and brittle as A15 compounds. Figure 21 illustrates T_c, B_{c2} (4.2 K), ρ_n and VHN (Vickers Hardness Number) of pseudo-binary V_2Hf_x Zr_{1-x} system [39]. The highest B_{c2} (4.2 K) of ~24 T is obtained at x = 0.55, which is nearly as high as that of Ti-doped Nb_3Sn. The upper critical field rapidly increases with decreasing temperature reaching ~30 T at 1.7 K. At x =0.55 the VHN of V_2Hf_x Zr_{1-x} is 440 which is less than half of that of A15 compounds.

Multifilamentary V_2(Hf, Zr) wires were fabricated from a composite of V matrix and Zr-Hf alloy cores. Addition of 1 at% Hf to the V matrix improves the hardness balance between the matrix and the cores. Figure 22 shows the cross-section of a 1425-core V_2(Hf, Zr) wire [40]. After the heat treatment at ~1000^{0}C, V_2(Hf, Zr) Laves phase layers are synthesized by diffusion between the matrix and the cores. Figure 23 shows the overall J_c versus magnetic field curves of 1425-core V_2(Hf, Zr) wires with

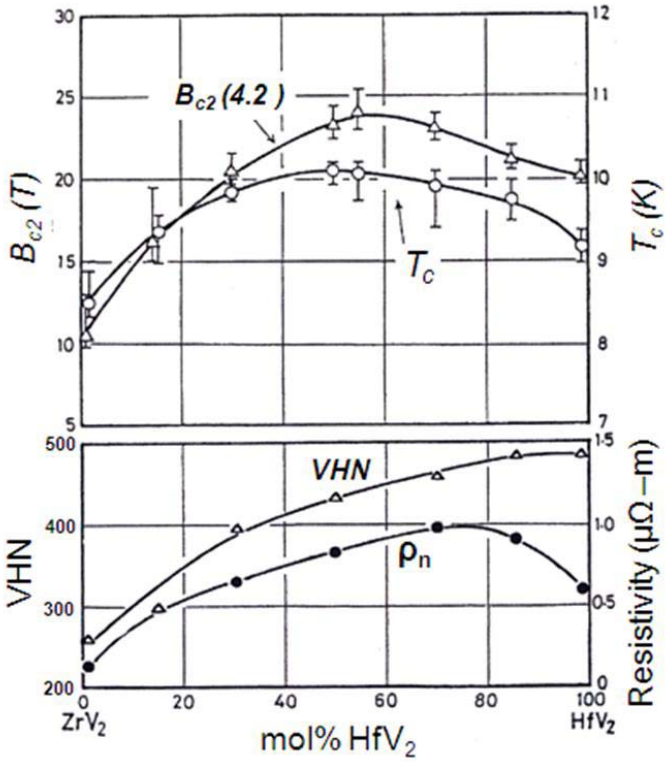

Fig.21. T_c, B_{c2} (4.2 K), normal state resistivity ρ_n and Vickers hardness in the pseudo-binary C15 compound $V_2Hf_xZr_{1-x}$ as a function of mole percent V_2Hf [39].

different core compositions [40]. An overall J_c of ~200 A/mm^2 is obtained at 4.2 K and 15 T for the Zr = 45~50 at% Hf core wire. The J_c of Laves phase layer may be one order larger than this value since its areal fraction in the wire is about 10 %. Stabilizing Cu may be clad on the wire since the heat treatment temperature is lower than the melting point of Cu.

The critical current of V_2(Hf, Zr) wire does not degrade at all under the tensile strain up to 0.55 % [41]. Moreover the T_c of the Laves type compound shows almost no degradation against the neutron irradiation [42]. The V_2(Hf, Zr) wires attracted interest for applications in fusion and accelerator magnets due to their superior strain and irradiation performance combined with high-field performance equivalent to that of Nb_3Sn wires.

Finally, the fabrication of Nb_3Ga, Nb_3Ge, V_3Si, NbN and Chevrel type $PbMo_6S_8$ compounds has been studied in Japan using different processes as summarized in refs. [43] and [44]. Each of these compounds has some distinct advantageous performance features. However, long length wires have not been fabricated.

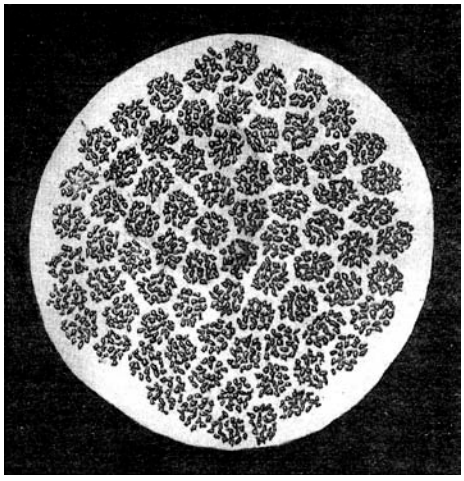

Fig.22. Cross-section of 1425-core V_2(Hf, Zr) wire with V-1at%Hf matrix and Zr-45at%Hf core [40].

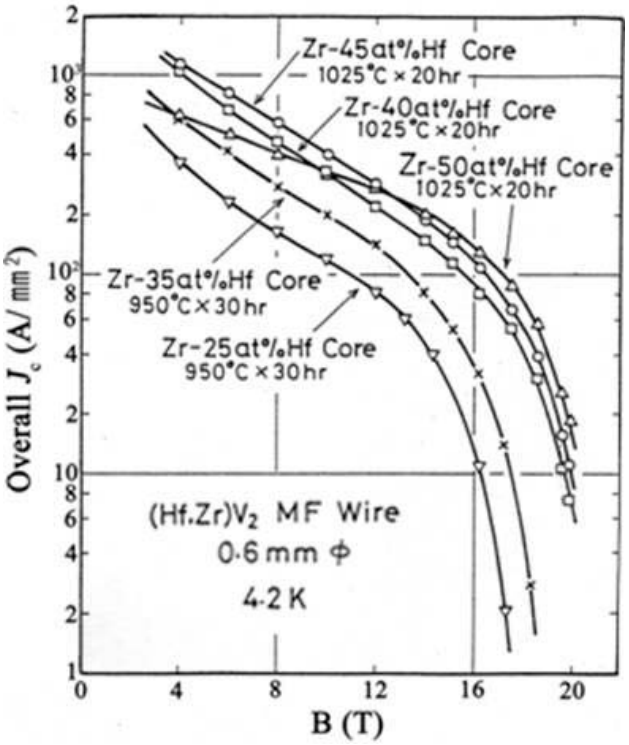

Fig.23. Overall J_c versus magnetic field curves for the V_2(Hf, Zr) wire with Zr-Hf cores of different compositions [40].

V. MgB_2 WIRES

A. Material Aspects

Since the discovery of superconductivity at 39 K by Prof. Akimitsu's group in 2001, MgB_2 has attracted much interest due to its potential to be used in liquid H_2 as well as to its simple combination of constituent elements [45]. The crystal structure of MgB_2 is a lamination of hexagonal Mg planes and B planes shown in Figure 24. Mg atoms locate at the center of B planes in the MgB_2 crystal. The coherence length of MgB_2 in the ab plane at 4.2 K is ~7 nm, long enough for the intrinsic inter-grain connectivity unlike in cuprate superconductors. The B_{c2} of MgB_2 is relatively low considering its high T_c of ~39 K. The B_{c2}(0 K) in the ab plane is ~15 T, while that in the perpendicular direction is ~5 T ; the anisotropy factor in B_{c2} is thus 3 – 4.

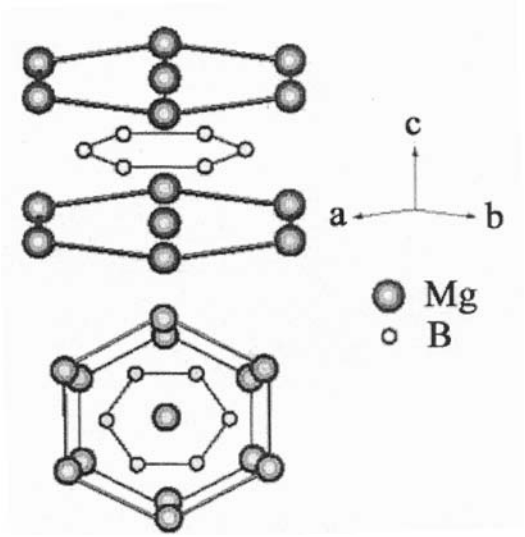

Fig.24. Crystal structure of MgB_2 [45].

The B_{c2} of MgB_2 increases significantly in films or by C doping as suggested by irreversibility field B_{irr} data in Figure 25 [46]. C is substituted in the B site which results in an appreciable decrease in T_c. The grain boundaries are considered to be the major flux pining centers in MgB_2, like in the A15 compounds described in Section II. Finer grain size is preferable to enhance the reaction between Mg and B. However finer grains tend to contain more oxygen. MgO layers formed on the MgB_2 surface deteriorate the connectivity of MgB_2 grains. Powder of MgH_2 used as Mg source is useful for reducing the amount of MgO surface layers [47]. The MgB_2 synthesis via the reaction $Mg + 2B \rightarrow MgB_2$ is accompanied by the volume reduction of ~30%, which also reduces the connectivity of the MgB_2 grains. A few fabrication processes

for MgB_2 wires studied in Japan are briefly described in the following sections.

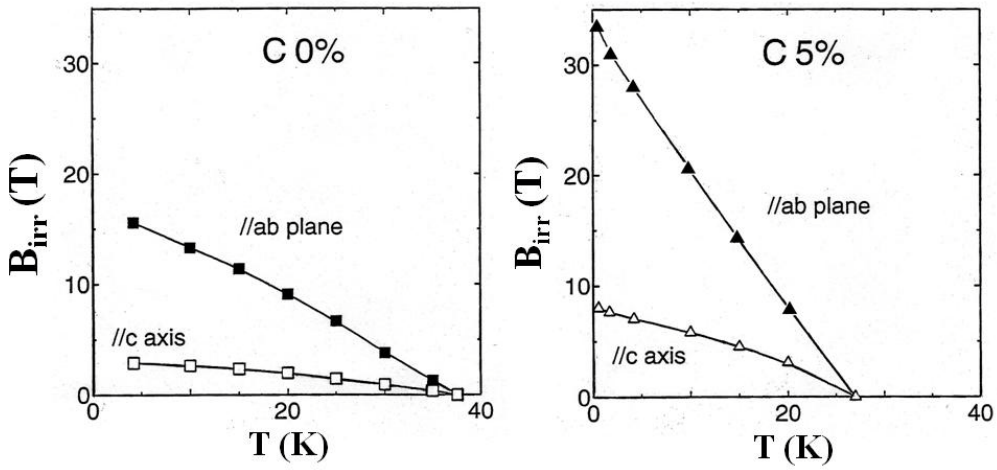

Fig.25. Effect of C substitution for B on the irreversibility field B_{irr} of MgB_2 single crystals. The anisotropy in the B_{irr} of MgB_2 about the direction of applied field is also illustrated [46].

.

B. Ex Situ Process

The *ex situ* process uses previously reacted MgB_2 powders filled into appropriate sheath tubes which are then fabricated into a wire [48]. The J_c of MgB_2 tapes depends on the sheath material as shown in Figure 26 [49]. Harder sheath yields better packing factor in the rolled tape thus improving the connectivity of MgB_2 grains. Figure 26 indicates that the anisotropy in J_c with respect to the direction of applied field becomes more significant in higher fields, which may be attributed to the anisotropy in B_{c2} indicated in Figure 25.

Grain connectivity is the most important factor in the J_c of MgB_2 tapes. At Tokai University we found that the J_c of *ex situ* MgB_2 tape is appreciably improved by a small amount of In addition [50]. Indium penetrates along MgB_2 grain boundaries by the heat generated during the rolling and the subsequent annealing at 200℃. The grain connectivity may be improved by the proximity effect in penetrated In. The mechanical tolerance of MgB_2 tape is also appreciably improved by the In addition. Finally, the performance of *ex situ* tapes strongly depends on the quality of starting MgB_2 powder. Nakane *et al*. reported a significant improvement of J_c in *ex situ* MgB_2 tape by using MgB_2 powder synthesized in the core of *in situ* tape as shown in Figure 27 [51]. The J_c of the tape is much improved compared to the conventional *ex situ* tape. Furthermore, in higher fields the J_c of the tape exceeds that of *in situ* processed tape; this may be due to the anisotropy illustrated in Figure 26.

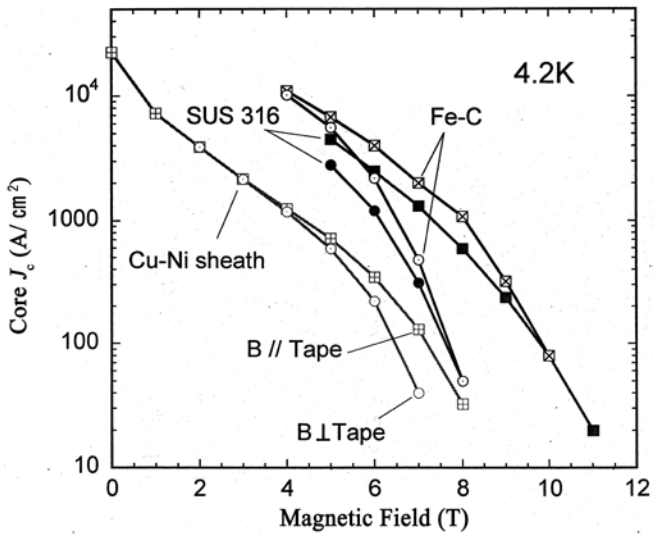

Fig.26. Anisotropy in J_c versus magnetic field curves of *ex situ* processed MgB_2 tapes with different sheath materials. The magnetic field is applied parallel (∥) and perpendicular (⊥) to the tape surface [49].

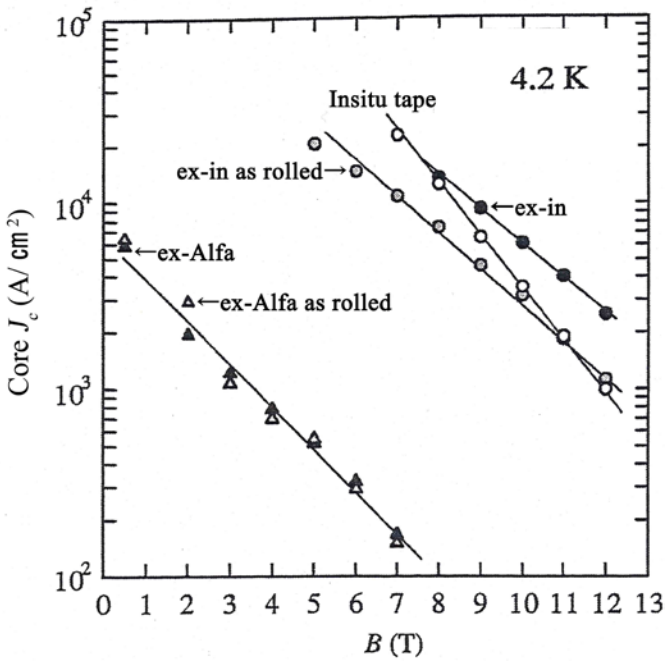

Fig.27. J_c versus magnetic field curves of *ex situ* processed MgB_2 tapes: ex-Alfa: *ex situ* tape using commercial MgB_2 powder from Alfa Aesor (325mesh, 99% purity), ex-in: *ex situ* tape using MgB_2 powder taken from the core of *in situ* processed tape [51].

C. In Situ Process

In the *in situ* process, a mixture of Mg and B powders is encased in a sheath tube, and after the wire fabrication the MgB_2 core is synthesized *in situ* by the heat treatment. Figure 28 illustrates the J_c (core) versus magnetic field curves of *in situ* processed MgB_2 tapes with C doping [52]. Tapes of MgB_2 were prepared from a powder mixture of MgH_2 powder and amorphous B. The C doping was performed using SiC nanopowder as well as different organic substances such as benzene (C_6H_6), ethyltoluene (C_9H_{12}) and thiophene (C_4H_4S). The mixed powder with C addition was ball-milled under a high purity argon gas for 1h. The mixed powder was filled in a Fe tube and fabricated to a tape. Figure 28 indicates that the addition of SiC or an organic substance improves J_c. A SiC addition improves the J_c in higher fields over that obtained by adding organic substances. The simultaneous addition of 10 mol% SiC and ethyltoluene further raises J_c in significant way. A J_c (core) of ~300 A/mm^2 has been obtained at 4.2 K and 10 T.

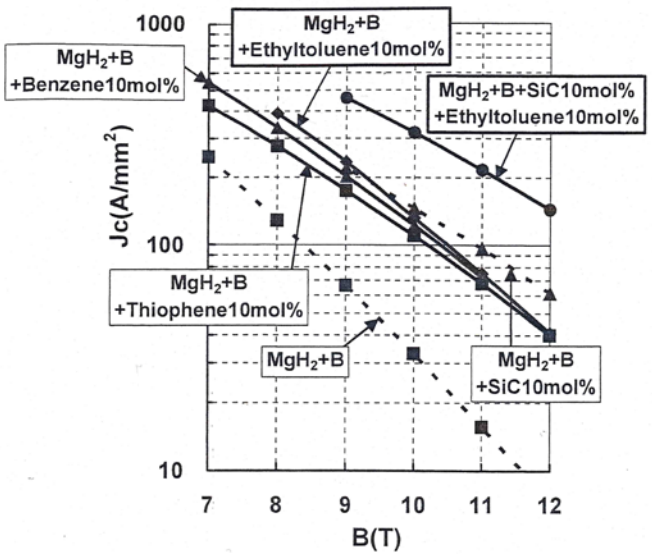

Fig.28. Magnetic field dependence of core J_c at 4.2K for organic substance and/or SiC powder added MgB_2/Fe tapes heat treated at 600℃ for 1h [52].

Generation of voids is observed in the *in situ* processed MgB_2 core due to the volume shrinkage associated with the Mg + 2B → MgB_2 reaction described before. Yamada *et al*. found that the heat treatment under uniaxial pressure reduces the voids thus improving the grain connectivity [53]. The areal fraction of MgB_2 core reduces nearly 40 % by the 100 MPa uniaxial pressure applied during the heat treatment at 630℃, which may be due to both the elimination of voids and the increase of packing factor in the core. Figure 29 illustrates the scanning electron

micrograph of the cross-section of MgB_2 core after the heat treatment with or without hot pressing. Appreciable densification of the core is observed after the hot pressing thus resulting in the improvement in J_c. A J_c of 440A/mm^2 has been obtained at 4.2 K and 10 T in the *in situ* tape with SiC and ethyltoluene addition.

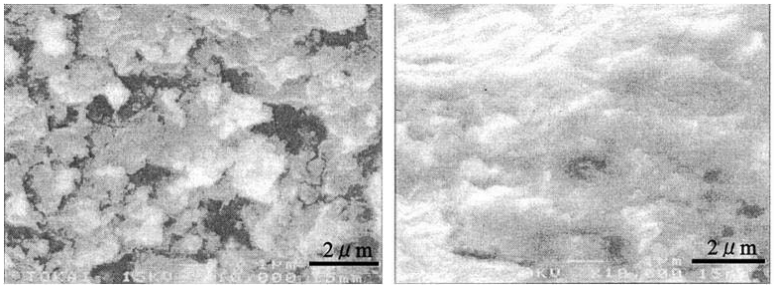

Fig.29. SEM structure on the cross-section of *in situ* MgB_2 tape. (a) Heat treated at 630℃ for 10h, (b) heat treated at 630℃ for 10h under 100MPa. [53]

Hitachi Ltd. and Central Japan Railway Co. developed long length MgB_2 wires through the *in situ* process. Tanaka *et al*. fabricated many 100 m-long mono-core wires with inner/outer sheath of Fe/Cu, Nb/Cu, Ta/Cu and Ta/Cu-Ni. These wires were wound into solenoid test coils [54]. Allowable bending strain after the reaction at 600℃ for 1 h was 0.5 – 0.7 %. Figure 30 shows the I_c at 4.2 K and 6 T of short samples and coils with different amount of SiC powder addition. The I_c of short samples and wires is significantly improved by the SiC addition. The coiled wires with 2.5 at% SiC and 5 at% SiC addition maintain the I_c of short samples. The J_c (core) of the coiled wires reaches ~500 A/mm^2 at 4.2 K and 6 T. However, the I_c of the coiled

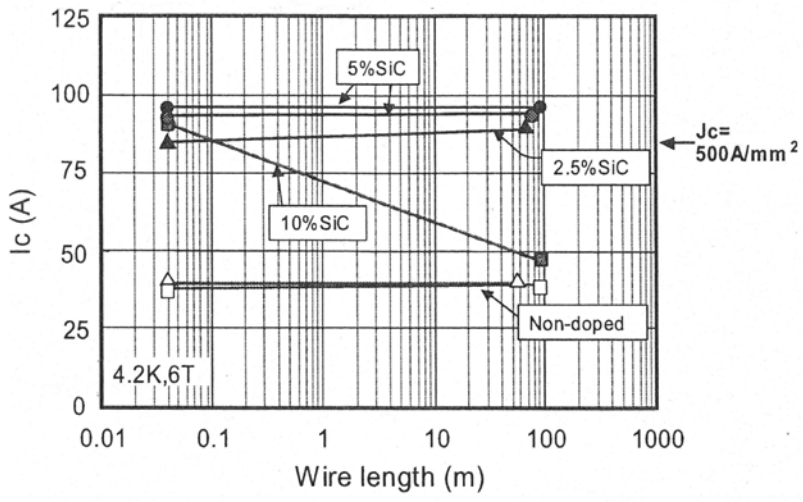

Fig.30. Critical current at 4.2K and 6T versus length of MgB_2 wires doped with different amount of SiC [54].

wire with 10 at% SiC addition shows an appreciable degradation indicating a longitudinal inhomogeneity in the wire. Takahashi *et al*. developed in Hitachi a persistent current switch (PCS) using a MgB_2 wire, and succeeded in the persistent current operation of 600 A for several hours in a circuit with this switch [55].

D. Diffusion Process

In this process, a dense MgB_2 layer is formed by the diffusion of Mg into B. When Mg is located inside B we have internal diffusion process while Mg outside B means external diffusion process. Figure 31 is an example of the cross-section of a 7 filaments internal diffusion processed wire [56]. Wires with 19 filaments were made in the analogous way. To create filaments, Mg rods were placed in holes drilled in the Ta sheath, and then the spaces between the rod and the sheath were filled with B powder containing the 5 mol% SiC addition. After the first drawing step, the Ta sheath with seven filaments was stacked in the Cu-Ni sheath, and again drawn into a wire. After the heat treatment at 640℃ for 1 h, MgB_2 layers 10 – 20 μm thick were synthesized. The Mg diffusion into the surrounding B layer produced a hole at the center of each filament as seen in Figure 31 (b). A J_c (MgB_2) of nearly 1000 A/mm^2 is obtained at 4.2 K and 10 T, which far exceeds that of *ex situ* or *in situ* processed wires, in the 19 filaments internal diffusion processed MgB_2 wire [56].

In the external diffusion process, B powder is filled in a Mg pipe with outer Fe sheath. The composite was at first groove-rolled and then drawn into a wire. Figure 32 (a) and (b) are the transverse and the longitudinal cross-section of the wire after the drawing [57]. A square shape of the Mg tube is visible in Figure 32 (a), due to the

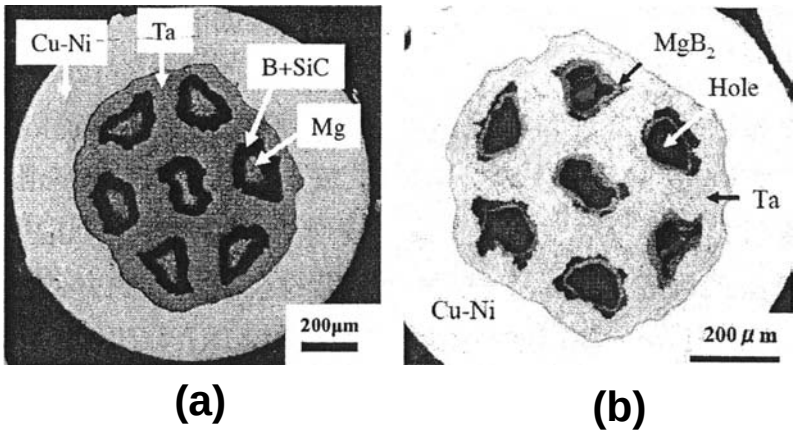

Fig.31. Cross-section of a MgB_2 wire with 7 filaments prepared by the internal diffusion process. (a) As drawn, (b) after the heat treatment at 640℃ for 1h [56].

effect of the groove-rolling. After the heat treatment at 630℃ for 10 h, MgB_2 core is synthesized as shown in Figure 32 (c). A small amount of residual Mg is observed at the square corners. A gap is observed around MgB_2 core after the heat treatment, which may be produced by the Mg diffusion as well as by the volume shrinkage in the MgB_2 formation. A J_c (MgB_2) of ~400 A/mm^2 is obtained at 4.2 K and 10 T in the external diffusion processed wires [57].

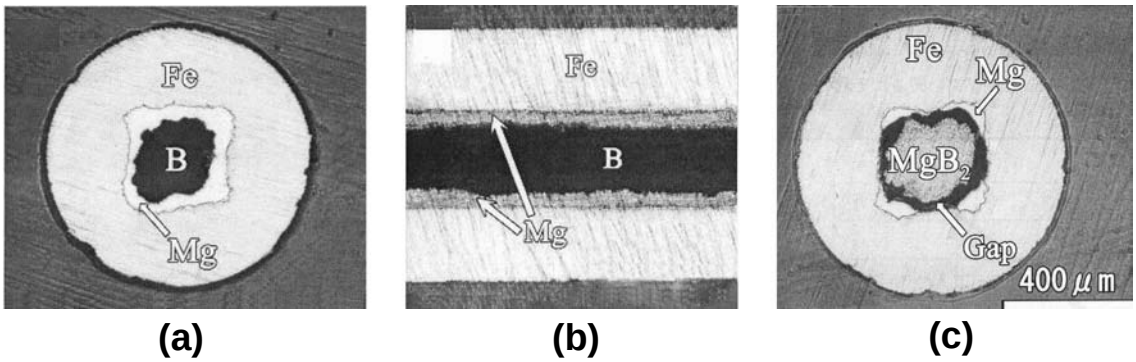

Fig.32. Cross-section of a monocore MgB_2 wire prepared by the external diffusion process using a Mg pipe and a Fe sheath. (a) Transverse cross-section, (b) longitudinal cross-section, (c) transverse cross-section after the heat treatment at 630℃ for 10h [57].

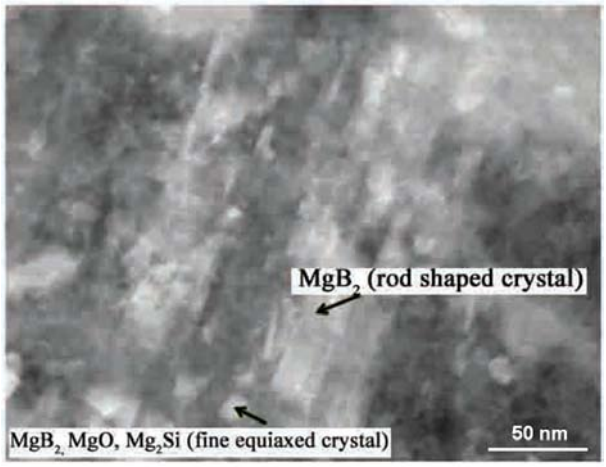

Fig.33. An image of low-angle annular dark-field scanning transmission electron microscope taken on the MgB_2 layer formed in the wire shown in Fig.31 [58].

That the diffusion process yields a larger J_c (core) than the *ex situ* and *in situ* process may be due to the better connectivity of MgB_2 grains. Figure 33 is a transmission electron micrograph of the MgB_2 layer formed in the internal diffusion processed wire shown in Figure 31[58]. MgB_2 grains are relatively small 10 – 100 nm in diameter. Figure 33 suggests a better connectivity of MgB_2 grains than that reported for the *in situ* processed wire [59]. A further improvement in J_c may be expected in

the MgB_2 wire prepared by the diffusion process through the optimization in the cross-sectional design. However, a wire with long length has not yet been fabricated by the diffusion process.

VI. CONCLUSIONS

The development of metallic superconductors in Japan has been initiated a couple of years behind that in the USA. Nevertheless, Japan soon became one of the world leaders, both in R&D and in manufacturing of metallic superconductors. The fabrication technologies of Nb-Ti and Nb_3Sn wires have been well established in the first half of 1980's, before the discovery of high-T_c cuprates in 1986-87. Basic studies based on material science and fabrication technology supported the continuing progress.

Mass production of Nb-Ti wires by procedures using the combination of drawing and intermediate annealings has been gradually optimized, starting from high homogeneity alloy ingots. Nb-Ti wires will be continuously used throughout the world due to their low price and easy handling.

The Nb_3Sn wires have opened new application areas above 10T becoming one of the key materials in science and technology. The bronze process produces fine filamentary wires with small AC loss. The internal Sn process yields higher J_c originated from the larger amount of Sn in the matrix. More detailed studies of processing parameters may still yield further progress in Nb_3Sn wires.

Long length Nb_3Al wires have been fabricated by the continuous RHQT process which reconciles stoichiometry with fine grains. Nb_3Al wires show slightly higher J_c than Nb_3Sn wires at 20T. Further improvement in high-field performance of Nb_3Al wires may be expected by ternary additions.

MgB_2 wires have a potential to be used in liquid H_2 coolant. This is a major advantage over other metallic superconductors. However, J_c of MgB_2 is still lower than that of Nb-Ti and Nb_3Sn wires due to the poor connectivity between grains. Improved powder quality, fabrication techniques and dopants may enhance the J_c of MgB_2 wires. The development of MgB_2 wires is still underway.

The development of metallic superconductors has a history half a century long. However, they still show potential for improvement of their performance. Metallic superconductors will enjoy longevity as a base of application technologies due to the easy mass production and reliable performance.

RERERENCES

[1] J.E. Kunzler, "Superconductivity in High Magnetic Fields at High Current Densities", *Rev. Modern Phys*., **33** 501-509 (1961).

[2] *High Magnetic Fields*, eds. H. Kolm, B. Lax, F. Bitter and R. Mills; Technol. Press, Cambridge, Mass., (1962).

[3] K. Tachikawa and B. Okai; "Metallurgical aspects and superconducting current capacities of Nb-Zr alloys", *J. Jpn. Inst. Metals*, **28** 16-21 (1964) (in Japanese).

[4] T. Shimada, *et. al*., "Manufacturing of superconducting cable for the LHC-key technology and statistical analysis", *IEEE Trans. Appl. Supercond*. **12** 1075-1078 (2002).

[5] Linear Guide, JR Tokai (September 2009).

[6] K. Matsumoto *et al*., "Enhanced J_c properties in superconducting Nb Ti composites by introducing Nb artificial pins with a layered structure", *Appl. Phys. Lett*. **64** 115-117 (1994).

[7] K. Miyashita, K. Sugiyama, S. Sakai, K. Kamata and H. Chiba, "Nb-Ti superconducting strands with Cu-Ni-Mn matrix and 2kA-class cables for AC use", *Proceedings ICEC16/ICMC*, eds. T. Haruyama, T. Mitsui and K. Yamafuji; Elsevier Science, Oxford, pp. 1851-1854 (1997).

[8] N. Yanagi and A. Iwamoto, "Development and fabrication of superconducting helical coils for LHD －Development of superconductors for the helical coils of LHD", *J. Cryogenic Soc. Japan* **32** 563-572 (1997) (in Japanese).

[9] A. Yamamoto *et. al*., "Design and development of the ATLAS central solenoid magnet", *IEEE Trans. Appl. Supercond*., **9** 852-855 (1999).

[10] H. Okuno *et. al*.; "The superconducting ring cyclotron in RIKEN", *IEEE Trans. Appl. Supercond*., **17** 1063-1068 (2007).

[11] A. Yamamoto, M. Nozaki and T. Yoshida, "Bess-Polar: Search for primordial antiparticle by long duration balloon flights at Antarctica", *BUTSURI* (published by The Physical Soc, Japan) **58** 86-93 (2003) (in Japanese).

[12] K. Tachikawa and Y. Tanaka,"Superconducting critical current of V_3Ga wires made by a new diffusion process", *Jpn. J. Appl. Phys*. **6** 782 (1967).

[13] K. Tachikawa, Y. Tanaka and S. Fukuda, Japanese Patent 0670619 (Filed June 25, 1966).

[14] K. Tachikawa, Y. Tanaka, K. Inoue, K. Itoh and T. Asano, "17.5 Tesla superconducting magnet", *J. Cryogenic Soc. Japan* **11** 252-257 (1976) (in Japanese).

[15] K. Tachikawa, "Studies on superconducting V_3Ga wire", *Proceedings ICEC-3*, Iliffe Sci. & Technol. Pub. , Surrey, UK 339-340 (1970).

[16] Y. Furuto, T. Suzuki, K. Tachikawa and Y. Iwasa, "Current-carrying capacities of superconducting multifilamentary V_3Ga cables", *Appl. Phys. Lett*. **24** 34-36 (1974).

[17] E. Nembach and K. Tachikawa," An electron microscope investigation of the flux pinning centers in

superconducting V_3Ga tape", *J. Less-Common Metals* **19** 359-367 (1969).

[18] Y. Hashimoto, K. Yoshizaki and M. Tanaka, "Processing and properties of superconducting Nb_3Sn filamentary wires", *Proc. ICEC-5*, ed. K. Mendelssohn; (1974) 332-335.

[19] Osaka Alloying Works, private communication (2011).

[20] H. Sekine, Y. Iijima and K. Tachikawa, "Composite-processed Nb_3Sn superconductors with titanium addition to the matrix", *J. Appl. Phys.* **53** 5354-5356 (1982).

[21] E. Helfand and N.R. Werthamer, "Temperature and purity dependence of the superconducting critical field-Ⅱ", *Phys. Rev*. **147** 288-302 (1966).

[22] S. Foner, E.J. McNiff Jr., G.M. Ozeryancky and R.E. Schwall, "High field properties of multifilamentary $(Nb\text{-}4at\%Ta)_3Sn$", *IEEE Trans. Magn*. **MAG-3** 984-987 (1987).

[23] T. Kiyoshi *et.al*., "Operation of a 930 MHz high-resolution NMR magnet at TML", *IEEE Trans. Appl. Supercond*. **15** 1330-1333 (2005).

[24] R. Hirose et. al., "Development of 15T cryogen-free superconducting magnet", *IEEE Trans. Appl. Supercond*. **16** 953-956 (2006).

[25] K. Okuno, H. Nakajima and N. Koizumi, "From CS and TF model coils to ITER : lessons learnt and further progress", *IEEE Trans. Appl. Supercond*. **16** 880-885 (2006).

[26] Y. Takahashi et. al., "Status of procurement for ITER superconductors", *Abst. Conf. Cryogenic Soc. Japan*, **81** 49 (2009) (Nov. 2009, Okayama) (in Japanese).

[27] K. Tachikawa, K. Miyashita, K. Sugiyama, *et al*., "2T-class 50Hz AC magnet of 50mm-bore made by bronze-processed submicron filament new Nb_3Sn cables", *Proc. ICEC 17*, eds. D. Dew-Hughes, R. G. Scurlock and J.H.P Watson; IOP, Bristol, 439-442 (1998).

[28] Y. Kubo *et.al*., "Superconducting properties of Nb_3Sn wires with radially arranged filaments", *IEEE Trans. Appl. Supercond.* **16** 1232-1236 (2006).

[29] K. Tachikawa, T. Ando, H. Sasaki, M. Yamaguchi and T. Takeuchi, "Structure and performance of Nb_3Sn superconducting wires prepared from Sn-based alloy sheets", to be published in *IEEE Trans. Appl. Supercond*. **21** (2011).

[30] S. Ceresara, M.V. Ricci, N. Saccheti and G. Sacerdoti; "Nb_3Al formation at temperatures lower than 1000℃", *IEEE Trans. Magn.* **MAG-11** 263-265 (1975).

[31] Y. Yamada *et al*., "Development of Nb_3Al superconductors for International Thermonuclear Experimental Reactor (ITER)", *Cryogenics* **39** 115-122 (1999).

[32] N. Koizumi *et al*., "Critical current test results of 13T-46kA Nb_3Al cable-in-conduit conductor", Cryogenics **42** 675-690 (2002).

[33] H. Kumakura, K. Togano, S. Tsukamoto, H. Irie and K. Tachikawa, "Structure and superconducting properties of Nb_3Al and $Nb_3(Al, Ge)$ composite tapes prepared by electorn beam irradiation", *J. Japan Inst. Metals* **51** 465-471 (1987) (in Japanese).

[34] K. Togano, H. Kumakura, T. Takeuchi and K. Tachikawa, "$Nb_3(Al, Ge)$ superconductors prepared by

hot-substrate liquid-quenching and subsequent annealing", *IEEE Trans. Magn*. **MAG-19** 414-417 (1983).

[35] T. Takeuchi, K. Togano and K. Tachikawa,"Nb_3Al and its ternary A15 compound conductors prepared by a continuous liquid quenching technique", *IEEE Trans. Magn*. **MAG-23** 956-959 (1987).

[36] T. Takeuchi *et al*, "Status and perspective of the Nb_3Al development", *Cryogenics* **48** 371-380 (2008).

[37] R. Yamada *et al*, "Feasibility study of Nb_3Al Rutherford cable for high field accelerator magnet application", *IEEE Trans. Appl. Supercond*. **17** 1461-1463 (2007).

[38] K. Inoue and K. Tachikawa, "Upper critical field of superconducting Laves phase in V-Hf-X ternary alloys", *Proc. 1972 Appl. Supercond. Conf.* , IEEE Pub 72 CFO 682-TABSC 415-418 (1972).

[39] K. Inoue and K. Tachikawa, "Structures and superconducting properties of the composite-processed Laves phase type V/Hf_xZr_{1-x}", *J. Japan Inst. Metals* **39** (1975) 1274-1282 (in Japanese).

[40] K. Inoue, T. Kuroda and K. Tachikawa, "Superconducting properties of V_2(Hf, Zr) Laves phase multifilamentary wires", *J. Nuclear Materials* **133&134** 815-818 (1985).

[41] K. Inoue, H. Wada, T. Kuroda and K. Tachikawa, "Stress effects on superconducting properties of the composite-processed V_2(Hf, Zr)", *Appl. Phys. Lett*. **38** 939-941 (1981).

[42] B. S. Brown, J. W. Hafstrom and T. E. Klippert, "Changes in the superconducting critical temperature after fast-neutron irradiation", *J. Appl. Phys*. **48** 1759-1761 (1977).

[43] K. Tachikawa, "Metallic Superconductors - part-5", *J. Cryogenic Soc. Japan*, **45** 387-397 (2010) (in Japanese).

[44] K. Tachikawa, "Metallic Superconductors - part 6", *J. Cryogenic Soc. Japan*, **45** 470-483 (2010) (in Japanese).

[45] J. Nagamatsu, N. Nakagawa, T. Muranaka, Y. Zenitani and J. Akimitsu, "Superconductivity at 39K in magnesium diboride", *Nature* **410** 63-64 (2001).

[46] E. Ohmichi, T. Masui, S. Lee, S. Tajima and T. Osada, "Enhancement of irreversibility field in carbon-substituted MgB_2 single crystal", *J. Phys. Soc. Jpn*. **73** 2065-2068 (2004).

[47] H. Fujii, K. Togano and H. Kumakura, "Enhancement of critical current densities of powder-in-tube processed MgB_2 tapes by using MgH_2 as a precursor powder", *Supercond. Sci. Technol*. **15** 1571-1576 (2002).

[48] G. Grasso, A. Malagoli, C. Ferdeghini, *et al*., : Appl. Phys. Lett. **79** 230-232 (2001).

[49] H. Kumakura, A. Matsumoto, H. Kitaguchi and H. Hatakeyama, "Critical current densities of powder-in-tube (PIT) processed MgB_2 tapes", *Materials Trans*. **45** 3056-3059 (2004).

[50] K. Tachikawa, Y. Yamada, O. Suzuki, M. Enomoto and M. Aodai, "Effect of metal powder addition on the critical current in MgB_2 tapes", *Physica* **C 382** 108-112 (2002).

[51] T. Nakane, H. Kitaguchi and H. Kumakura, "Improvement in the critical current density of *ex situ*

powder in tube processed MgB_2 tapes by utilizing powder prepared from an *in situ* processed tape", *Appl. Phys. Lett*. **88** 022513-1 - 022513-3 (2006).

[52] H. Yamada, N. Uchiyama, A. Matsumoto, H. Kitaguchi and H. Kumakura, "The excellent superconducting properties of *in situ* powder-in-tube processed MgB_2 tapes with both ethyltoluene and SiC powder added", *Supercond. Sci. Technol*. **20** L30-L33 (2007).

[53] Y. Yamada, M. Nakatsuka, K. Tachikawa and H. Kumakura, "Effect of carbide addition and hot pressing on superconducting properties of *in-situ* PIT-processed MgB_2 tapes", *J. Cryogenic Soc. Japan* **40** 493-497(2005) (in Japanese).

[54] K. Tanaka, M. Takahashi, M. Okada, *et al*., "Fabrication and transport properties of insitu/PIT processed wires and coils", J. Cryogenic Soc. Japan **41** 519-524 (2006) (in Japanese).

[55] M. Takahashi, K. Tanaka, M. Okada, H. Kumakura and H. Kitaguchi, "Development of persistent current switch made with MgB_2 wire", *J. Cryogenic Soc. Japan* **41** 525-530 (2006) (in Japanese).

[56] K. Togano, J. Hur, A. Matumoto and K. Kumakura, "Fabrication of internal Mg diffusion processed MgB_2 wires－influence of filament size on structure and properties", *Abst. Conf. Cryogenic Soc. Japan*, **82** 118 (2010) (May 2010, Kawasaki) (in Japanese).

[57] T. Hori, K. Wada, Y. Yamada, K. Tachikawa and H. Kumakura, "Superconducting properties and structure of MgB_2 wires prepared by diffusion process using Mg rod and tube", *Abst. IUMRS-Int. Conf. Asia 2008, 228 (BBP-6)* (Dec. 2008. Nagoya).

[58] Y. Shimada, Y. Kubota, S. Hata, *et. al*., "Microstructure in high-density MgB_2 wires prepared by an internal Mg diffusion method", to be published in IEEE Trans. Appl. Supercond. vol 21 (2011).

[59] Y. Zhu, A. Matsumoto, B.J. Senkowicz, *et al*., "Microstructure of SiC nano particle-doped MgB_2 / Fe tapes", *J. Appl. Phys*. **102** 013913-1－013913-9 (2007).